3

Disparate cervical trauma in low severity insults

Saami J. Shaibani

Associate Professor of Physics
Department of Mathematics
Liberty University
Lynchburg, VA 24506

This paper was presented at the 19th Annual Workshop on Human Subjects for Biomechanical Research. It has not been screened for accuracy nor refereed by any body of scientific peers and should not be referenced in the open literature.

Abstract

Detailed analyses were made of real-world collisions between a bullet vehicle and a stationary target vehicle, whose subsequent motion was less than 15 kilometers per hour. Calculations were performed to determine the forces generated in the lower neck and the upper neck of restrained occupants in the target vehicles. The values obtained were compared with known tolerances so that the likelihood of neck injury could be assessed. These results were complemented by clinical examinations of the occupant, which gave additional insight into the relationship between the impact (cause) and the trauma (effect). The small values for the former, and their limited range, produced considerable variations in the latter. Such anomalies suggest that the severity of injury cannot always be found by considering apparently similar cases; instead, the outcome may sometimes only be revealed by evaluating the circumstances of the individual case.

1. Introduction

The human neck is an immensely complicated structure that can be damaged in a wide variety of ways, ranging from impact-induced trauma to degenerative effects of *inter alia* arthritis or old age. A pathological examination of tissue from the neck may not always be able to distinguish between different modes of damage, and other approaches are called for. Among the latter, observations made during surgery may provide useful indications of the mechanisms responsible for the tissue damage but this may require the surgeon to concentrate on secondary issues when his primary duty is to attend to the delicate surgical procedures usually involved. Thus, conventional assessments can fail to shed light on particular mechanisms for cervical trauma.

The research described in this paper offers a new approach to understanding cervical trauma in the case of vehicle occupants. The main technique in this approach is the calculation of the forces within the lower neck and the upper neck by using a recent microcomputer version[1-2] of a computer model, which was developed for the study of impact events[3-12]. (Superscripted numbers in brackets denote references at the end of the paper.) The calculated forces are then compared with experimental data on human tolerance values, and these physical quantities are reviewed in the context of the previous medical history of the occupants of interest to this study. The new methodology developed here is completed by integrating the above aspects of it with clinical examinations of the occupants, thereby connecting the trauma with the insult.

2. Methodology

The kinematics of the occupant in each of the stationary target vehicles in this study were modeled by the Crash Victim Simulation (CVS) program. This is a computer program which models the response of a multi-segmented body to an impact, or other insult, in geometrically definable surroundings. Typically, the body is an anthropomorphic test device (ATD) or "dummy", the insult is a passenger vehicle crash pulse and the surroundings are a passenger vehicle compartment. The program was developed at the Calspan Corporation, Buffalo, New York, in the 1970s for use on mainframe computers and, as such, it was primarily a tool for advanced research[3-12]. This limited status was transformed in the early 1980s when CVS was first adapted successfully by the author for use in the minicomputer environment at the University of Oxford, England, where major progress was made in expanding the accessibility of CVS[13-19]. More recently, a microcomputer version of CVS, which is known as the SJSATBPC package and which gives mainframe-quality results, has been developed[1-2].

The first truly rigorous reconstructions of occupant kinematics were undertaken for various types of accident at the University of Oxford[17-19]. Only complicated real-world accidents were chosen for that research because straightforward accidents could be explained more readily by other means. Brief details of two of the former are: (a) a head-on collision of a subcompact vehicle with a change in speed of about 32 to 40 kilometers per hour (kph) [20 to 25 miles per hour (mph)][17], in which an unrestrained front seat passenger died; and, (b) an oblique impact at about 30 degrees anticlockwise from the forward direction (in England, this goes from the driver on the right side of the passenger compartment towards the front seat passenger on the left) of a subcompact vehicle with a change in speed in excess of 64 kph [40 mph][18-19], in which an unrestrained driver survived. These accidents were non-trivial because both of them superficially contradicted common sense, in that death was considered unlikely in case (a) but almost certain in case (b).

It was only the great care taken in the above studies that enabled the causes of trauma to be identified, as follows. For case (a), the contact forces were typical for that type of accident, but the dashboard geometry caused those forces to be highly concentrated. This led to large pressures in the region of the chest, resulting in fractures of several ribs and the sternum, damage to both lungs, and a rupture of the aorta. Hence, a nominally survivable accident ended in a fatality. For case (b), the right side of the chest struck the left side of the steering wheel, causing the body to rotate clockwise and to the right. The head hit the windshield, and the left knee (but not the right knee) impacted the dashboard with a force well in excess of 10 kilonewtons (kN) [one ton]. The rotational motion of the body was transmitted to the left leg in such a way that, coupled with the longitudinal load along the length of the femur, the left hip was dislocated without fracture. (The absence of fracture to either the pelvis or the femur was most unusual.) The chest injury was assigned a score of AIS = 4, the head AIS = 3, and the lower leg AIS = 3, where AIS refers to the Abbreviated Injury Scale[20-21]. This distribution of injuries managed the energy of the impact in a remarkably even manner so that a nominally fatal accident was survived.

The successful application of the minicomputer version of CVS, as described above, was also seen with the SJSATBPC version of CVS when the same deliberate treatment was adopted for an accident in which the use or non-use of a seat belt was a central issue[22-23]. The key to this case was the energy management of the impact by the body, which sustained injuries to the head, chest and both legs. The emergency room physician examining the vehicle occupant identified the major trauma as a hemothorax, for which a value of AIS = 5 may be assigned, and there was a minor injury of a broken tooth with AIS = 1. (The demise of the vehicle occupant within an hour or so of admission to the emergency room, without recovering consciousness, suggests that the value of AIS = 5 could almost be viewed as AIS = 6.) The extent of the leg injury was deduced from an inspection of the two dents in the vehicle dashboard, corresponding to the points of impact of the knees. Equivalent physical quantities defined in Federal Motor Vehicle Safety Standard (FMVSS) 208[24-30] for these three injuries give values of the order of: head injury criterion (HIC) = 300 [say], chest severity index (CSI) = 70 g [say] where g is the acceleration due to gravity at the surface of the earth, and leg load = 400 pounds (lbf) [say]. The best match in Table 2.1 with these scores is seen at 20 mph with no belt worn, with all other comparisons providing at least one inconsistency and therefore reinforcing the result.

It should be noted that all of the preceding studies avoided the errors that can be made during the less comprehensive methodologies employed by others.

Table 2.1

Distribution of injuries incurred in a frontal pole impact[22-23] calculated by the Crash Victim Simulation (SJSATBPC version)

change in speed Δv (mph)	slack in belt (in)	HIC	CSI (g)	force on legs (lbf)
15	0	66	16	0
	3	39	23	18
	6	27	27	204
	no belt	24	26	237
20	0	254	46	0
	3	139	50	9
	6	158	81	117
	no belt	288	76	406
25	0	251	63	0
	3	507	98	25
	6	363	150	388
	no belt	369	183	460

3. Physical measurements

3.1 Determination of impact environment

There are many standard techniques for capturing relevant engineering data at the scene of an accident[31-36], but the circumstances surrounding the two particular collisions investigated in this study are so simple that a more basic appraisal can be made.

(A) Rear impact at stop sign. A stationary subcompact vehicle at a stop sign was struck in the rear by a second subcompact vehicle. An assessment of the damage to the two vehicles, coupled with the statements made by the occupants of the vehicles, produced a peak-to-peak velocity of 8.0 kph [5.0 mph] to 13.5 kph [8.5 mph] for the struck vehicle. The use of this velocity parameter is explained in Appendix A.

(B) Side impact at minor intersection. A stationary subcompact vehicle at a minor intersection was struck a glancing blow by the front left bumper of a second subcompact vehicle, which was approaching from the left and turning right towards the struck vehicle. The striking vehicle was not affected by the impact, and the only damage to the struck vehicle was a small indentation on the forward part of the door panel near the A pillar on the driver's side. The deformed area was roughly circular, measuring approximately 20 centimeters (cm) [8 inches (in)] in diameter and having a penetration depth of less than 5 cm [2 in], which is consistent with the struck vehicle experiencing a peak-to-peak velocity of not more than 8 kph [5 mph].

3.2 Values for CVS input data

The CVS input data for the above two cases of interest to this study were developed in the following manner:

Occupant. A common practice of using a standard 50th percentile dummy, with a mass of 75 kilograms (kg) [165 pounds (lb)] and a height of 178 cm [70 in], was followed for both the rear impact and the side impact described in the previous section. This is acceptable here because the main purpose of this research was to deduce the overall level for the forces within the neck. The marginal benefit (if any) from using a dummy with exactly the same characteristics as the vehicle occupant was outweighed by the extra complication involved in employing a non-standard dummy. The use of a standard dummy is denoted by the letter "N" as the first character in the eight-character label for the CVS input data, in accordance with the system of nomenclature defined elsewhere[1]. An outline of the nomenclature is shown in Table 3.1.

Table 3.1

Nomenclature of eight-character label for description of CVS input data[1]

#	meaning	suggestion	example
1	type of occupant	first letter of name or mnemonic	A: Sierra C: child E: Euler Part572 F: female H: Hybrid III L: 95th percentile N: non-Euler Part572 P: pedestrian S: side impact
2	magnitude of insult	0.1 x Δv, or rate of rollover ω (# of 1/4 turns/sec)	0: $0 < \Delta v < 9$ 1: $10 < \Delta v < 19$ etc 0: $0.0 < \omega < 0.9$ 1: $1.0 < \omega < 1.9$ etc
3	direction of insult	direction of clock, or polarity and center of rollover	1, 2, .. 9, A, B & C L: -ve @ left side M: -ve @ middle N: -ve @ right side P: +ve @ left side Q: +ve @ middle R: +ve @ right side
4	vehicle geometry	first letter of make	(implied)
5	vehicle property	supplement to #4	(e.g. vehicle model)
6	restraint system	type of belt and airbag	0: none 1: two-pt shoulder 2: two-pt lap 3: three-pt A: airbag only B: airbag + 2-pt lap C: airbag + 3-pt
7,8	variation	consecutive	01, 02, 03, ...

Impact. An account of how a stationary vehicle can move from its original position, and then return to rest, is given in Appendix A for the rear impact and in Appendix B for the side impact. An end point of 200 milliseconds was set for the CVS calculations, although results toward the end of this timeframe may sometimes need to be treated with some caution. Two values -- 8.0 kph [5.0 mph] and 13.5 kph [8.5 mph] -- were chosen for the peak-to-peak velocity in the rear impact to cover the range explained in the previous section. For the side impact, the realistic figure of 8 kph [5 mph], derived as an upper limit in the previous section, and an exaggerated figure of 13 kph [8 mph], were used. The latter was included so that the most extreme range of impact severities could be entertained. In both impacts, the two velocities are distinguished by the numbers "0" and "1" as the second characters in the label for the CVS input data.

The angle of the side impact was calculated from photographic evidence of the struck vehicles and from measurements made of an exemplar vehicle. A range of - 60° to - 50° (denoting angles anticlockwise from the forward direction) was ascertained as being the closest to the actual angle, which could not be identified unambiguously because of the uncertainty in the variable location of the driver's seat. The recommendations for labeling the third character can be modified slightly to represent the lower and upper boundaries in the above range by "A" and "B", respectively. The rear impact simply has "6" as the third character.

Geometry. The passenger compartment in exemplars of the vehicles involved in this study was measured, and the subsequent triangulations gave a configuration that was consistent to within less than 2.5 cm [one inch]. Minor adjustments were made to reflect the curvatures of the seat cushion and of the seat back, and the presence of carpets on the floorboard. The fourth and fifth characters of the CVS input data label were assigned the letters "SW" in the rear impact and "CC" in the side impact. The reported use of the three-point belt supplied to the vehicles is denoted by the value of "3" as the sixth character for both impacts.

Properties. The functions describing force-deflection, inertial spike, energy absorption factor, deflection factor, and coefficient of friction were taken from the known characteristics of similar vehicles, including other subcompacts.

Allowed contacts. These were set to the obvious values applicable to the occupant-vehicle interaction.

Position. The initial seating position of the occupant was based on a detailed inspection of an exemplar vehicle. In addition, the orientations of each part of the occupant were such that they were physiologically consistent with human postures in automotive environments.

A summary of how the above six sets of CVS input data are labeled appears in Table 3.2.

Table 3.2

Application of nomenclature for CVS input data labels to cases examined in this study

#	rear impact	side impact
1	N: non-Euler Part572	N: non-Euler Part572
2	0: 8.0 kph [5.0 mph] 1: 13.5 kph [8.5 mph]	0: 8 kph [5 mph] 1: 13 kph [8 mph]
3	6: 180 degrees	A: - 60 degrees B: - 50 degrees
4	S: Subaru	C: Chevrolet
5	W: wagon	C: Chevette
6	3: three-point belt	3: three-point belt
7,8	02	05

Hence, N06SW302, N0ACC305, N0BCC305, N16SW302, N1ACC305 & N1BCC305

4. Results

The calculations performed by CVS (SJSATBPC version) with the above input data were analyzed with particular regard to the responses at two joints within the occupant model, namely the neck pivot and the head pivot. The neck pivot may be referred to as the lower neck because it is located in the vicinity of the C6 and C7 vertebrae at the lower extremity of the cervical spine (see Figure 4.1[37]). Similarly, the head pivot may be referred to as the upper neck because it is located in the vicinity of the C1 and C2 vertebrae at the upper extremity of the cervical spine (again, see Figure 4.1).

The forces in the neck pivot and the head pivot may be assessed by considering their components along the x, y, z axes of conventional three-dimensional Cartesian space, resulting in six separate forces F[±x], F[±y] and F[±z]. The presence of a + or - sign indicates

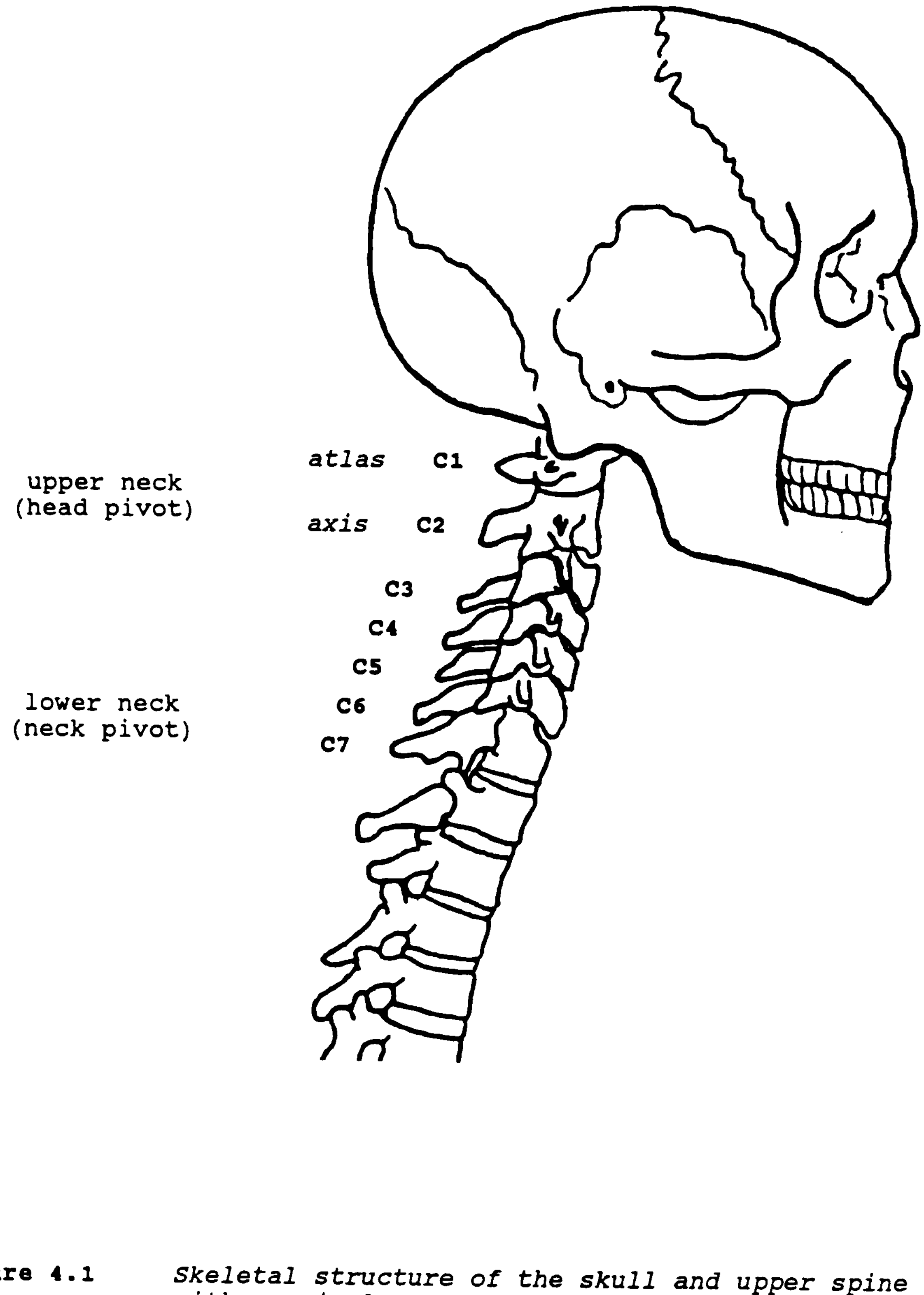

Figure 4.1 *Skeletal structure of the skull and upper spine with cervical vertebrae C1 to C7*

forces in a particular direction, whereas the notation F[x], F[y] and F[z] denotes the forces in both directions with a sense. The sense of x is taken to be along the anterior-posterior direction in the human body, that is the forward-rearward direction; the sense of y is along the left-right direction in the human body; and, the sense of z is along the superior-inferior direction in the human body, that is along the upward-downward direction. The forces within the xy plane can be considered as shear forces, whereas the force along z is axial with the positive direction being compressive and the negative direction being tensile.

The polarities for the negative and positive directions within the x, y and z senses depend on which frame of reference applies. There are multiple possibilities for this: (1) the local coordinate system of one of the two body segments which the joint connects, (2) the local coordinate system of the other body segment which the joint connects, and (3) the coordinate system of the inertial frame of reference. A survey of the ambiguities inherent in the above matrix of possibilities produces:

(a) F[z] is negative at the initial time t = 0 and, since one would expect the weight of the head to act downward before any insult has been applied, it appears that the positive z direction is upward;

(b) There is a small downward acceleration of the head and neck segments when the occupant has been seated by the equilibrium subroutine of CVS at the initial time, which is consistent with (a);

(c) F[x] is negative at the initial time and, since one would expect the body to lean slightly rearward into the seat back before any insult has been applied, it appears that the positive x direction is forward; and,

(d) There is a small rearward acceleration of the head and neck segments when the occupant has been seated by the equilibrium subroutine of CVS at the initial time, which is consistent with (c).

The above polarity for F[z] is opposite to the usual definition of vehicle geometry -- positive x forward, positive y to the right and positive z downward -- that has been adopted here as the inertial frame of reference. The polarity for F[y] may be determined from the "right hand rule" and then checked with the lateral component of the occupant motion after the initial time.

The next two sections contain an overview of the forces generated in the neck for the six particular cases listed in Table 3.2. The temporal aspects of the data are omitted for the sake of clarity in the these two sections, but they are considered in the subsequent section.

4.1 Forces in the neck pivot (lower neck)

Values for F[±x], F[±y] and F[±z] in the neck pivot are presented in Table 4.1, where the units of force are the metric quantity, the newton (N), and the Imperial unit, the pound (lbf). A number of features in the table may be identified:

(a) peak-to-peak velocity v_{p-p} = 8 kph [5 mph]

(1) F[x] for each impact are greater than F[y] and F[z].

(2) F[x] and F[z] for the rear impact N06SW302 are greater than for the two side impacts N0ACC305 and N0BCC305.

(3) The forces for both side impacts are generally comparable, although N0BCC305 has a greater F[-x] while N0ACC305 has a slightly greater F[-y].

(4) All three impacts have roughly similar values for F[y].

(b) peak-to-peak velocity v_{p-p} = 13 kph [8 mph]

(5) As in (1) above.

(6) As in (2) above.

(7) The forces for both side impacts are generally comparable, although N1BCC305 has a greater F[+x] and F[+z] (cf. (3) above).

(8) F[x] and F[z] are greater at the higher speed than the lower speed for all impacts, but the values for F[y] are fairly similar.

(9) F[-x] for the rear impact N16SW302 is much larger than any other F[x].

(10) F[+z] for the rear impact N16SW302 is much larger than any other F[z].

These results, and those in the next two sections, will be explored further in the discussion section.

Table 4.1

Maximum forces, in newtons (and pounds), within the neck pivot calculated by the Crash Victim Simulation (SJSATBPC version)

*(a) peak-to-peak velocity = 8 kph [5 mph]**

	N06SW302		N0ACC305		N0BCC305	
F[+x]	516	(116)	365	(82)	374	(84)
F[-x]	574	(129)	360	(81)	414	(93)
F[+y]	80	(18)	59	(13)	53	(12)
F[-y]	102	(23)	138	(31)	98	(22)
F[+z]	245	(55)	36	(8)	18	(4)
F[-z]	178	(40)	85	(19)	98	(22)

*(b) peak-to-peak velocity = 13 kph [8 mph]**

	N16SW302		N1ACC305		N1BCC305	
F[+x]	610	(137)	396	(89)	503	(113)
F[-x]	1224	(275)	503	(113)	485	(109)
F[+y]	178	(40)	71	(16)	45	(10)
F[-y]	107	(24)	151	(34)	147	(33)
F[+z]	405	(91)	59	(13)	223	(50)
F[-z]	200	(45)	174	(39)	156	(35)

* N06SW302, N16SW302 have v_{p-p} = 8.5, 13.5 kph [5.0, 8.5 mph]

4.2 *Forces in the head pivot (upper neck)*

The response of the head pivot is described in Table 4.2, which bears a strong resemblance to the response of the neck pivot in Table 4.1. In fact, all of the features noted in the previous section for the neck pivot can be used in a qualitative manner to characterize the head pivot. The overall similarity between the head pivot and the neck pivot is quite noticeable, but one quantitative difference exists:

(11) All F[x], F[y] and F[z] for each impact and peak-to-peak velocity are about ten per cent greater within the neck pivot than within the head pivot.

4.3 *Pictorial output from SJSVUEPC program*

Although the name SJSATBPC is used to denote the microcomputer version for CVS, there are in fact two programs in the SJSATBPC package: (a) the SJSCVSPC program, which is a microcomputer version of the actual CVS program, and (b) the SJSVUEPC program, which is a microcomputer version of an adjunct to the CVS program called the View program[38-39]. For simplicity, the generic term SJSATBPC often appears when SJSCVSPC is more accurate but SJSVUEPC is preferred when specific use of that program takes place. The results in this section are hard copy figures from the SJSVUEPC program at particular points in time, as illustrated in Figures 4.2 and 4.3 for the two rear impacts N06SW302 and N16SW302, respectively. The four side impacts are not shown here because the extent of the travel is less than that seen in the figures already depicted.

The number of time points that can be included in sequences similar to those included here is necessarily limited, and it may not always be possible to reveal the desired level of detail in the occupant kinematics. A useful modification of the SJSVUEPC program, called the SJSFLMPC program[2], allows sequences of multiple images produced by the SJSVUEPC program to be captured. Their subsequent animation display provides unique insights that cannot be obtained in any other way, as shown in the film[23] made for the hard copy figures in a similar study to this[22]. The success of this technique has been repeated for this study by making another film[40] with the SJSFLMPC program, which highlights the instances in time at which the forces listed in Tables 4.1 and 4.2 occur.

Table 4.2

Maximum forces, in newtons (and pounds), within the head pivot calculated by the Crash Victim Simulation (SJSATBPC version)

*(a) peak-to-peak velocity = 8 kph [5 mph]**

	N06SW302	N0ACC305	N0BCC305
F[+x]	445 (100)	312 (70)	329 (74)
F[-x]	512 (115)	303 (68)	356 (80)
F[+y]	71 (16)	49 (11)	45 (10)
F[-y]	89 (20)	116 (26)	85 (19)
F[+z]	218 (49)	31 (7)	18 (4)
F[-z]	151 (34)	76 (17)	85 (19)

*(b) peak-to-peak velocity = 13 kph [8 mph]**

	N16SW302	N1ACC305	N1BCC305
F[+x]	525 (118)	343 (77)	441 (99)
F[-x]	1077 (242)	441 (99)	418 (94)
F[+y]	160 (36)	58 (13)	40 (9)
F[-y]	93 (21)	125 (28)	116 (26)
F[+z]	356 (80)	53 (12)	196 (44)
F[-z]	174 (39)	151 (34)	134 (30)

* N06SW302, N16SW302 have v_{p-p} = 8.5, 13.5 kph [5.0, 8.5 mph]

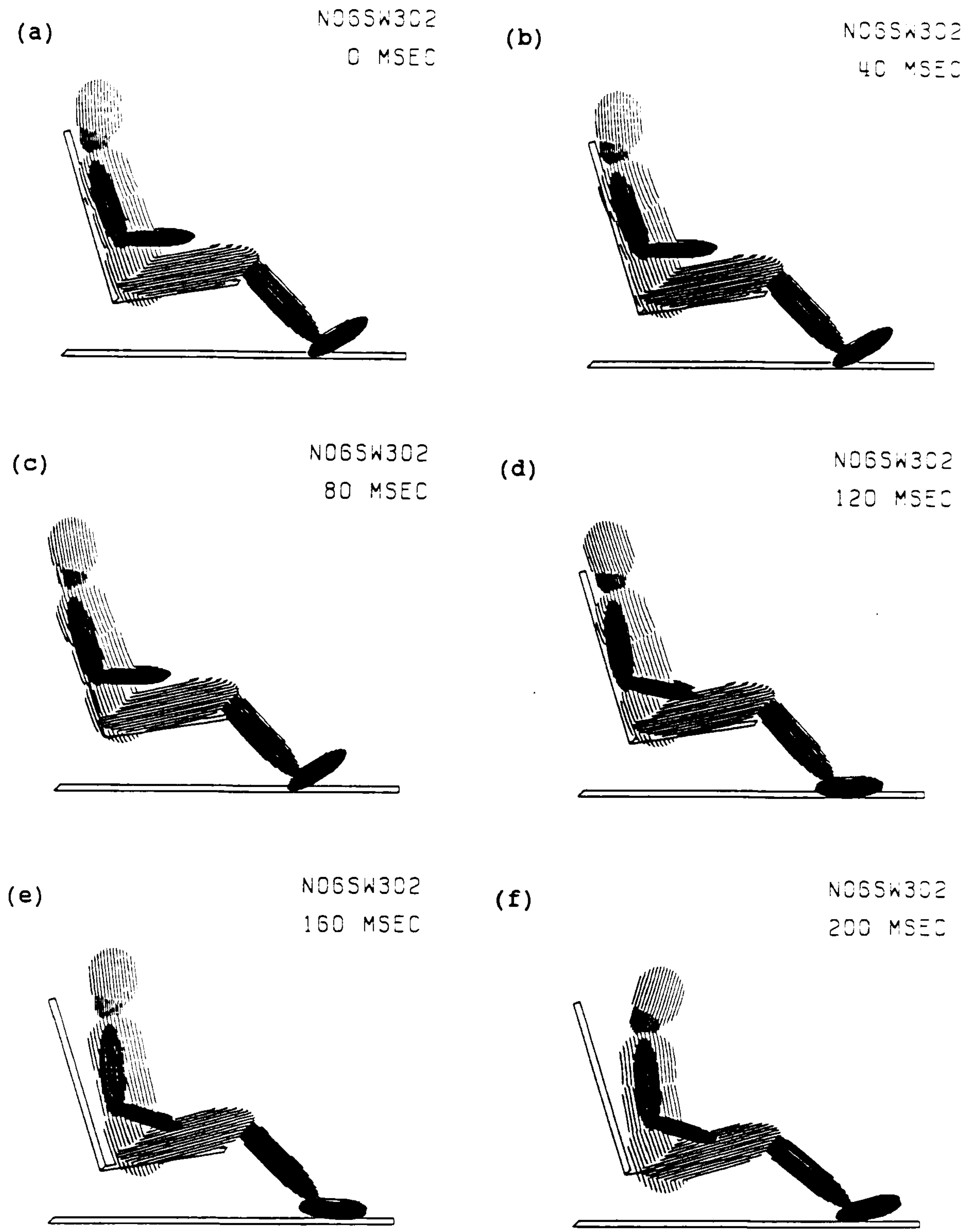

Figure 4.2 *Output from SJSVUEPC program for CVS input data N06SW302 at times t = (a) 0, (b) 40, (c) 80, (d) 120, (e) 160, and (f) 200 milliseconds*

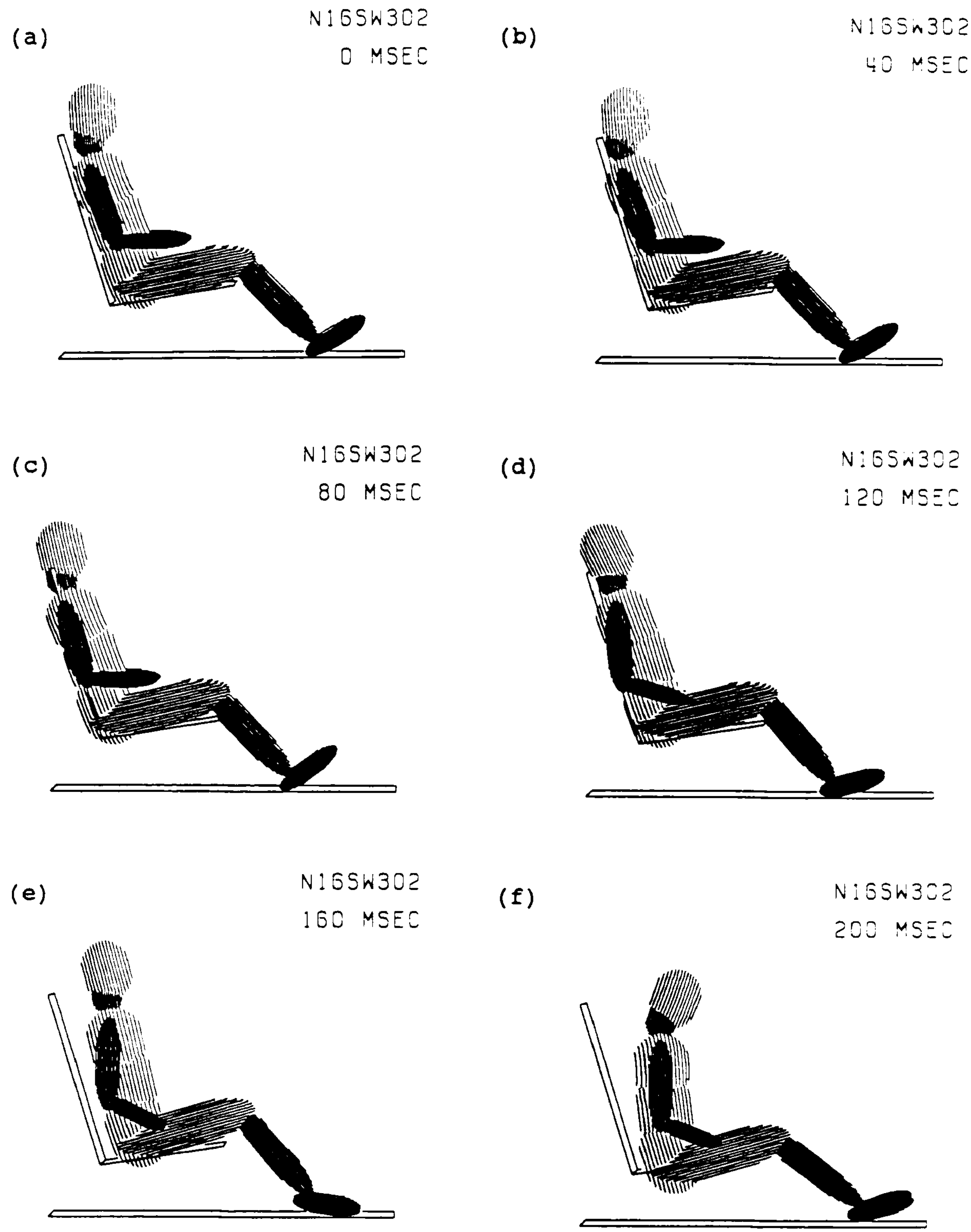

Figure 4.3 *Output from SJSVUEPC program for CVS input data N16SW302 at times t = (a) 0, (b) 40, (c) 80, (d) 120, (e) 160, and (f) 200 milliseconds*

5. Discussion

5.1 Explanation of neck forces

The results calculated in previous sections have established the general level of force generated in the lower neck (Table 4.1) and the upper neck (Table 4.2) of restrained vehicle occupants subjected to low severity insults in real-world accidents. A brief account of how the observations made earlier can be understood is now given for each of the features numbered (1) to (11) in the results section:

(1) The use of correctly fitted three-point lap and shoulder belts by a vehicle occupant can cause the torso to experience some significant changes in its motion. This is because the torso is constrained in the forward x direction by the belt and in the rearward x direction by the seat back. Consequently, the motion in the x sense will tend to be disturbed more than that in the y and z senses, where the constraints are not so limiting. This explains why F[x] are greater than F[y] and F[z] for all the cases in Tables 4.1 and 4.2.

(2) The rear impact N06SW302 is predominantly along the x sense, whereas the side impacts have components along the y sense. Thus, the former can be expected to have a greater F[x] which, in turn, can give greater extension and/or flexion and can thereby induce a greater F[z].

(3) An increase in the angle of side impact from N0BCC305 to N0ACC305 can cause a reduction in F[x], and an accompanying increase in F[y], because a more lateral impact reduces the forward-rearward motion and increases the left-right motion.

(4) The value of F[y] in a rear impact can be expected to be less than that in a side impact, as seen in (3). However, the greater F[x] in a rear impact in (2) can induce a greater F[y] in the same way that F[z] was increased in (2). This increase of F[y] in a rear impact can make it comparable to that in a side impact.

(5) As in (1) above.

(6) As in (2) above.

(7) A more frontal side impact can produce a greater F[x], as seen in (3), and this can lead to a greater F[z], as seen in (2).

(8) An increase in the peak-to-peak velocity of an impact can be expected to give an increase in all F[x], F[y] and F[z]. The increases in the forces cannot necessarily be

expressed as a function of the peak-to-peak velocity because the energy of the impact is dissipated throughout the whole vehicle/occupant environment. In particular, the main bulk of the body -- especially the interaction of the torso with the belt and seat back -- will respond in a different way to the extremities. The similar values of F[y] at both peak-to-peak velocities may be due to the interdependence of F[x], F[y] and F[z], as mentioned in (2) and (4).

(9) F[x] tend to be greater than F[y] and F[z], as seen in (1); in addition, a rear impact produces a greater F[x], as seen in (2). This increase in F[x] can be compounded by a high rebound from the seat back in the forward direction, giving an even higher value of F[-x].

(10) The elevated value of F[x] in (9) can induce a similarly elevated F[z], which is upward and therefore F[-z].

(11) When other factors are equal, the response of the torso may tend to affect the lower neck more than the upper neck because the lower neck is directly coupled with the torso. The different motion of the torso in (8) and its more immediate effect on the lower neck may explain why all of the maximum forces within the lower neck in Table 4.1 are about ten per cent greater than the corresponding values within the upper neck in Table 4.2.

A perspective on the range of forces in Tables 4.1 and 4.2 is given in Table 5.1 by values from a very low severity full frontal impact with v_{P-P} = 3 kph [2 mph], which were calculated recently in a separate study of an unrestrained occupant.

5.2 Human tolerances

Two standard reference works on human tolerances[41-42] summarize some major studies on the response of the neck in human volunteer tests[43-45]. The experiments conducted in these studies were static in nature, and the measurements reported were reactions at the occipital condyles (Table 5.2). The data in the table do not represent the threshold of damage but, rather, a limit of comfort which may be short of pain or damage. Although the testing methodology for determining data on human tolerances cannot be related directly to the impact environments examined in this research, there is still merit in invoking those data for general comparison purposes, as shown below.

An inspection of the forces in Tables 4.1, 4.2 and 5.1 shows that only one of the seven impacts examined in this study has a neck force that exceeds the tolerances in Table 5.2, namely F[-x] in the

Table 5.1

Maximum forces, in newtons (and pounds), for input data N0CFE001 calculated by the Crash Victim Simulation (SJSATBPC version)

	neck pivot		head pivot	
F[+x]	85	(19)	76	(17)
F[-x]	36	(8)	36	(8)
F[+y]	0	(0)	0	(0)
F[-y]	0	(0)	0	(0)
F[+z]	see note 1		see note 2	
F[-z]	85	(19)	76	(17)

1. F[z] < 0 for all t with a least negative value of 31 N (7 lbf).
2. F[z] < 0 for all t with a least negative value of 27 N (6 lbf).

Table 5.2

Tolerances for the human neck, in newtons (and pounds)

F[+x]	posterior-anterior	845	(190)
F[-x]	anterior-posterior	845	(190)
F[+y]	right-left lateral	400	(90)
F[-y]	left-right lateral	400	(90)
F[+z]	axial tension	1134	(255)
F[-z]	axial compression	1112	(250)

higher speed rear impact N16SW302. (It should be noted that the location of the upper neck may correspond more closely to the occipital condyles than the lower neck, and therefore provide a better basis of comparison.) This does not necessarily mean that there was definitely an injury in that case, or that there was definitely no injury in the other six cases, because factors such as age, height, weight, gender, and health have not been included. When such factors are taken into account, it does indeed appear that the higher speed rear impact had a high probability of injury whereas the other six impacts did not.

There is a chance that a pre-existing medical condition of the occupant in the side impact may have effectively lowered the values in Table 5.2 to the extent that an otherwise low probability of injury was increased enough to suggest some risk of damage to the neck. (Details of that condition included a fusion of the C4 and C5 cervical vertebrae.) However, the values for the very low severity full frontal impact in Table 5.1 seem so low that only a major medically-related reduction would allow any significant probability of injury to arise.

6. Conclusions

The occupant kinematics of vehicle occupants in a variety of low severity real-world collisions have been calculated by the SJSATBPC microcomputer version[1-2] of the Crash Victim Simulation[3-12]. The forces generated in the neck pivot (lower neck) and the head pivot (upper neck) of the occupants were evaluated and found to be quite different even though the insults associated with the collisions were quite similar. This is an important result because it shows that nominally comparable insults cannot always be assumed to produce similar injuries, especially in the neck region; instead, each individual case may need to be examined separately.

Comparisons of neck forces with human tolerance data[41-45] were made to determine the probability of cervical trauma. This exercise was undertaken in the light of clinical examinations of the vehicle occupants so that factors such as age and health could be included. The resulting correlation between the probability of neck injury and the cervical trauma assessed by clinical neurological examination provided a good match in the limited number of cases investigated in this research.

Appendix A

Functional forms for vehicular time histories in rear impacts

Any impact event may be divided into n parts, separated by the increasing time points $t = t_i$ for $i = 0, 1, 2, \ldots n$. Let the linear displacement s, linear velocity v, and linear acceleration a, at these times be called s_i, v_i and a_i, respectively. The boundary conditions for s, v and a in a general rear impact may be described by setting $n = 4$, and they are listed in Table A.1. If the changes in v are symmetrical about the time $t = t_2$, then

$$t_2 - t_0 = t_4 - t_2 = \tau/2 \qquad \text{(A.01)}$$

where

$$\tau = t_4 - t_0 \qquad \text{(A.02)}$$

is the period of the impact event. The initial time $t = t_0$ can be set to zero so that

$$t_2 = \tau/2 \qquad \text{(A.03)}$$

and $$t_4 = \tau \qquad \text{(A.04)}$$

If v is expressed as a function of t, the roots of v in Table A.1 occur when $t = t_0 = 0$ and $t = t_4 = \tau$. Both of these roots are repeated at least once because the derivative of v, namely a, is also zero at these t. As a starting point, let these roots be repeated just once (say). Now , if $t = 0$ (twice) and $t = \tau$ (twice) are roots of v, then t^2 and $(t - \tau)^2$ are factors of v. A simple combination of these factors is

$$v = k\, t^2\, (t - \tau)^2 \qquad \text{(A.05)}$$

where k is a constant.

The maxima and minima of v occur when its first derivative is zero and its second derivative is negative and positive, respectively. The times for these stationary points may be found to be

$$t = 0 \quad \text{for a local minimum} \qquad \text{(A.06a)}$$

$$t = \tau/2 \quad \text{for a local maximum} \qquad \text{(A.06b)}$$

Table A.1

Boundary conditions for linear displacement s, velocity v, and acceleration a, in a general rear impact

Time	Values	Notes
t_0	$s_0 = 0$	No impact has occurred
	$v_0 = 0$	
	$a_0 = 0$	
t_1	$a_1 = a_{MAX}$	Maximum acceleration to achieve maximum velocity
t_2	$v_2 = v_{MAX}$	Maximum velocity achieved
	$a_2 = 0$	
t_3	$a_3 = a_{MIN}$	Maximum deceleration to return to zero velocity
t_4	$s_4 = s_{MAX}$	Final position
	$v_4 = 0$	
	$a_4 = 0$	

$$t = \tau \quad \text{for a local minimum} \tag{A.06c}$$

Hence, the maximum and minimum values for v may be determined as

$$v_{MAX} = k\, \tau^4 / 16 \tag{A.07}$$

and $$v_{MIN} = 0 \tag{A.08}$$

The usual definition for the change in velocity during an impact event is the difference between the initial and final velocities

$$\Delta v = v_4 - v_0 \tag{A.09}$$

but this is zero for the impact described in Table A.1. The concept of a peak-to-peak value $v_{P\text{-}P}$ is now introduced to give an idea of the range for v as

$$\begin{aligned} v_{P\text{-}P} &= v_{MAX} - v_{MIN} \\ &= k\, \tau^4 / 16 \end{aligned} \tag{A.10}$$

This identity allows the constant k to be deduced as

$$k = 16\, v_{P\text{-}P} / \tau^4 \tag{A.11}$$

and so the final form for v is

$$v = 16\, v_{P\text{-}P}\, t^2\, (t - \tau)^2 / \tau^4 \tag{A.12}$$

The solution for the form of a is found from differentiation of equation (A.12)

$$\begin{aligned} a &= dv/dt \\ &= 32\, v_{P\text{-}P}\, t\, (t - \tau)\, (2t - \tau) / \tau^4 \end{aligned} \tag{A.13}$$

The stationary points for a are given by

$$t = (3 - \sqrt{3})\, \tau / 6 \quad \text{for a local maximum} \tag{A.14a}$$

$$t = (3 + \sqrt{3})\ \tau / 6 \quad \text{for a local minimum} \qquad \text{(A.14b)}$$

from which the corresponding values are

$$a_{MAX} = 16\ v_{P\text{-}P} \sqrt{3} / 9\tau \qquad \text{(A.15)}$$

and

$$a_{MIN} = -16\ v_{P\text{-}P} \sqrt{3} / 9\tau = -a_{MAX} \qquad \text{(A.16)}$$

These equal and opposite values for the extrema in a may be represented in the peak-to-peak acceleration by

$$a_{P\text{-}P} = a_{MAX} - a_{MIN} = 2\ a_{MAX}$$

$$= 32\ v_{P\text{-}P} \sqrt{3} / 9\tau \qquad \text{(A.17)}$$

The solution for the form of s is found from integration of equation (A.12)

$$s = \int v\ dt$$

$$= 8\ v_{P\text{-}P}\ t^3 (6t^2 - 15\tau t + 10\tau^2) / 15\tau^4 + c \qquad \text{(A.18)}$$

where c is a constant. The initial boundary condition for s in Table A.1, i.e. $s_0 = 0$ at $t = t_0 = 0$, means that the constant of integration is

$$c = 0 \qquad \text{(A.19)}$$

and the explicit form for s is

$$s = 8\ v_{P\text{-}P}\ t^3 (6t^2 - 15\tau t + 10\tau^2) / 15\tau^4 \qquad \text{(A.20)}$$

It can be shown that the only stationary points for s are points of inflexion so that

$$s_{MAX} = 8\ v_{P\text{-}P}\ \tau / 15 \quad \text{at } t = \tau \qquad \text{(A.21)}$$

and

$$s_{MIN} = 0 \quad \text{at } t = 0 \qquad \text{(A.22)}$$

The range of s is simply

$$s_{P\text{-}P} = s_{MAX} - s_{MIN}$$

$$= 8\ v_{P\text{-}P}\ \tau\ /\ 15 \qquad (A.23)$$

Two parameters that can often be obtained from physical measurements are $v_{P\text{-}P}$ and $s_{P\text{-}P}$, and other quantities of interest in the above equations may be expressed in terms of them. This is achieved in the following relationships

$$\tau = 15\ s_{P\text{-}P}\ /\ 8\ v_{P\text{-}P} \qquad (A.24)$$

and $$a_{P\text{-}P} = 256\ v_{P\text{-}P}^{2}\ \sqrt{3}\ /\ 135\ s_{P\text{-}P} \qquad (A.25)$$

where τ is derived directly from equation (A.23) and $a_{P\text{-}P}$ is found by combining equations (A.17) and (A.24).

A range of estimates for the peak-to-peak velocity in the rear impact of interest to this study is

$$v_{P\text{-}P} = 8.0\ \&\ 13.5\ \text{kph}\ \ [\ =\ 5.0\ \&\ 8.5\ \text{mph}\ ] \qquad (A.26)$$

The level of accuracy is appropriate to the circumstances involved, which may be satisfied here by half of one decimal place.

The two corresponding values of $s_{P\text{-}P}$ are

$$s_{P\text{-}P} = 20\ \&\ 40\ \text{centimeters (cm)} \qquad (A.27)$$

$$[\ =\ 8\ \&\ 16\ \text{inches (in)}\ ]$$

to the nearest 10 centimeters. The time histories of a, v and s may be generated by applying the values in equations (A.24), (A.26) and (A.27) to equations (A.13), (A.12) and (A.20). Graphical representations of these are depicted in Figure A.1 for the smaller value of $v_{P\text{-}P}$ and in Figure A.2 for the larger value of $v_{P\text{-}P}$. The duration of the former is seen to be

$$\tau = 170\ \text{milliseconds (msec)} \qquad (A.28)$$

in agreement with equation (A.24); similarly, the duration of the latter is

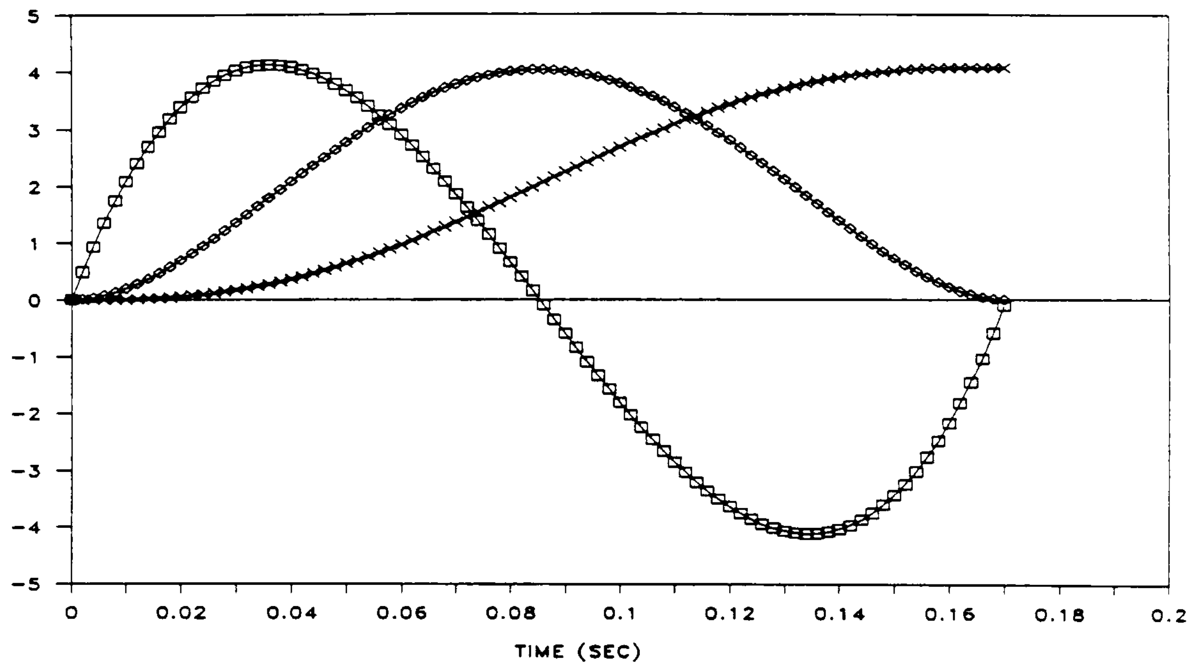

Figure A.1 *Time history for rear impact with v_{P-P} = 8.0 kph [5.0 mph]: (a) acceleration □, g; (b) velocity ◇, kph/2; and, (c) displacement ×, cm/5*

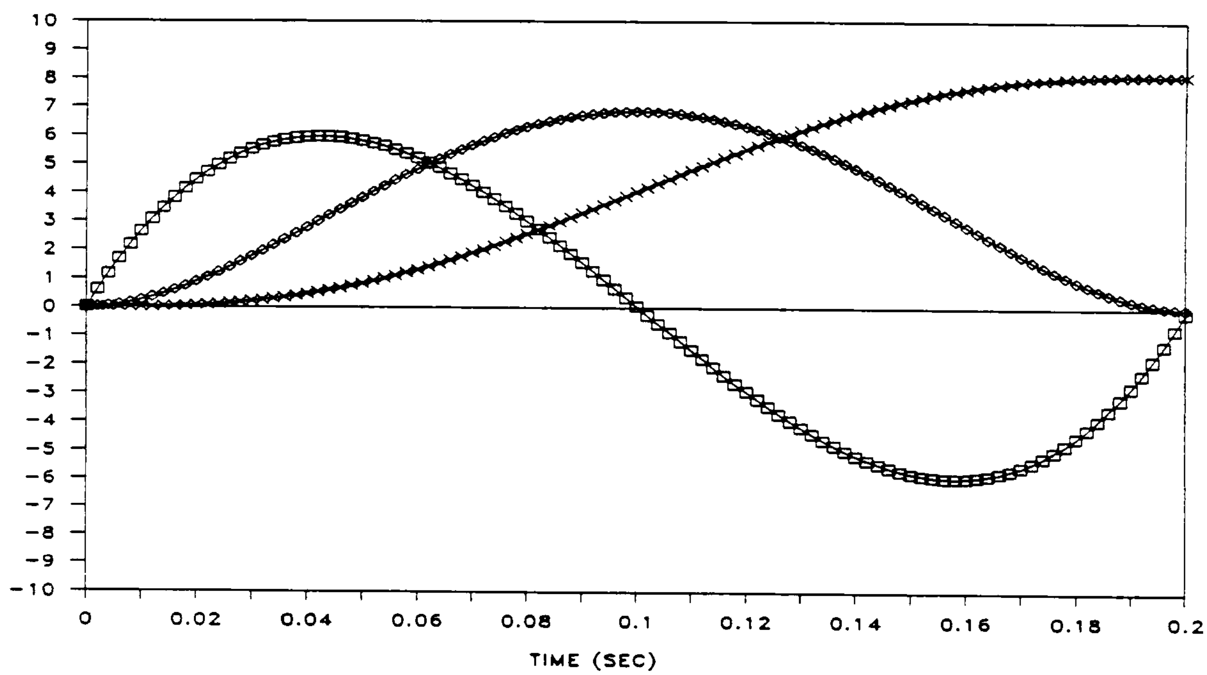

Figure A.2 *Time history for rear impact with v_{P-P} = 13.5 kph [8.5 mph]: (a) acceleration □, g; (b) velocity ◇, kph/2; and, (c) displacement ×, cm/5*

$$\tau = 201 \text{ msec} \tag{A.29}$$

The values of $a_{P\text{-}P}$ in Figures A.1(a) and A.2(a) coincide with calculations of equation (A.24) with equations (A.30) and (A.31), namely

$$a_{P\text{-}P} = 8.2 \ \& \ 11.9 \text{ g} \tag{A.30}$$

corresponding to $v_{P\text{-}P}$ = 8.0 and 13.5 kph, respectively. Here the appropriate accuracy is to one decimal place. The form of a in Figures A.1(a) and A.2(a) has

$$t[a_{MAX}] = 36 \text{ msec}; \quad t[a_{MIN}] = 134 \text{ msec} \tag{A.31}$$

$$\text{and} \quad t[a_{MAX}] = 42 \text{ msec}; \quad t[a_{MIN}] = 159 \text{ msec} \tag{A.32}$$

as the times of the extrema, respectively. These times match those derived from equation (A.14). As a further check with the latter, the sum of the times in equations (A.31) and (A.32) is found to be equal to the duration of the event in equations (A.28) and (A.29).

Appendix B

Functional forms for vehicular time histories in side impacts

Any impact event may be divided into n parts, separated by the increasing time points $t = t_i$ for i = 0, 1, 2, ... n. Let the linear displacement s, linear velocity v, and linear acceleration a, at these times be called s_i, v_i and a_i, respectively. The boundary conditions for s, v and a in a particular side impact may be described by setting n = 6, and they are listed in Table B.1. If the changes in v are symmetrical about the time $t = t_3$, then

$$t_3 - t_0 = t_6 - t_3 = \tau/2 \tag{B.01}$$

where

$$\tau = t_6 - t_0 \tag{B.02}$$

is the period of the impact event. The initial time $t = t_0$ can be set to zero so that

Table B.1

Boundary conditions for linear displacement s, velocity v, and acceleration a, in a given side impact

Time	Values	Notes
t_0	$s_0 = 0$	No impact has occurred
	$v_0 = 0$	
	$a_0 = 0$	
t_1	$a_1 = a_{MAX\#1}$	Maximum acceleration to achieve maximum velocity
t_2	$v_2 = v_{MAX}$	Maximum velocity achieved
	$a_2 = 0$	
t_3	$s_3 = s_{MAX}$	Maximum displacement and start of return to original position
	$v_3 = 0$	
	$a_3 = a_{MIN}$	
t_4	$v_4 = v_{MIN}$	Maximum negative velocity toward original position
	$a_4 = 0$	
t_5	$a_5 = a_{MAX\#2}$	Maximum acceleration to return to zero velocity
t_6	$s_6 = 0$	Original position
	$v_6 = 0$	
	$a_6 = 0$	

$$t_3 = \tau/2 \tag{B.03}$$

and $$t_6 = \tau \tag{B.04}$$

If v is expressed as a function of v, the roots of v in Table B.1 occur when $t = t_0 = 0$, $t = t_3 = \tau/2$ and $t = t_6 = \tau$. The first and last of these roots are repeated at least once because the derivative of v, namely a, is also zero at these t. As a starting point, let these roots be repeated just once (say). The non-zero value of a at t_3 means that this root of v is singular. Now , if $t = 0$ (twice), $t = \tau/2$ and $t = \tau$ (twice) are roots of v, then t^2, $(2t - \tau)$ and $(t - \tau)^2$ are factors of v. A simple combination of these factors is

$$v = - K t^2 (2t - \tau) (t - \tau)^2 \tag{B.05}$$

where K is a positive constant and the minus sign allows v to be positive, rather than negative, just after $t = 0$.

The maxima and minima of v occur when its first derivative is zero and its second derivative is negative and positive, respectively. The times for these stationary points may be found to be

$$t = 0 \quad \text{for a local minimum} \tag{B.06a}$$

$$t = (5 - \sqrt{5}) \tau / 10 \quad \text{for a local maximum} \tag{B.06b}$$

$$t = (5 + \sqrt{5}) \tau / 10 \quad \text{for a local minimum} \tag{B.06c}$$

$$t = \tau \quad \text{for a local maximum} \tag{B.06d}$$

Hence, the maximum and minimum values for v may be determined as

$$v_{MAX} = K \tau^5 \sqrt{5} / 125 \tag{B.07}$$

and $$v_{MIN} = - K \tau^5 \sqrt{5} / 125 = - v_{MAX} \tag{B.08}$$

The usual definition for the change in velocity during an impact event is the difference between the initial and final velocities

$$\Delta v = v_6 - v_0 \tag{B.09}$$

but this is zero for the impact described in Table B.1. The concept of a peak-to-peak value v_{P-P} is now introduced to give an idea of the range for v as

$$v_{P-P} = v_{MAX} - v_{MIN} = 2\ v_{MAX}$$
$$= 2\ K\ \tau^5 \sqrt{5}\ /\ 125 \qquad \text{(B.10)}$$

This identity allows the constant K to be deduced as

$$K = 25\ v_{P-P} \sqrt{5}\ /\ 2\tau^5 \qquad \text{(B.11)}$$

and so the final form for v is

$$v = -\ 25\ v_{P-P} \sqrt{5}\ t^2\ (2t - \tau)\ (t - \tau)^2\ /\ 2\tau^5 \qquad \text{(B.12)}$$

The solution for the form of a is found from differentiation of equation (B.12)

$$a = dv/dt$$
$$= -\ 25\ v_{P-P} \sqrt{5}\ t\ (t - \tau)\ (5t^2 - 5\tau t + \tau^2)\ /\ \tau^5 \qquad \text{(B.13)}$$

The stationary points for a are given by

$$t = (5 - \sqrt{15})\ \tau\ /\ 10 \quad \text{for a local maximum} \qquad \text{(B.14a)}$$
$$t = \tau/2 \quad \text{for a local minimum} \qquad \text{(B.14b)}$$
$$t = (5 + \sqrt{15})\ \tau\ /\ 10 \quad \text{for a local maximum} \qquad \text{(B.14c)}$$

from which the corresponding values are

$$a_{MAX} = 5\ v_{P-P} \sqrt{5}\ /\ 4\tau \qquad \text{(B.15)}$$

and $$a_{MIN} = -\ 25\ v_{P-P} \sqrt{5}\ /\ 16\tau = -\ (5/4)\ a_{MAX} \qquad \text{(B.16)}$$

These values for the extrema in a may be represented in the peak-to-peak acceleration by

$$a_{P-P} = a_{MAX} - a_{MIN} = (9/4)\ a_{MAX}$$

$$= \quad 45\ v_{P\text{-}P} \sqrt{5}\ /\ 16\tau \tag{B.17}$$

The solution for the form of s is found from integration of equation (B.12)

$$s \quad = \quad \int \ v\ dt$$

$$= \quad -\ 25\ v_{P\text{-}P} \sqrt{5}\ t^3\ (t\ -\ \tau)^3\ /\ 6\tau^5 \ +\ C \tag{B.18}$$

where C is a constant. The initial boundary condition for s in Table B.1, i.e. $s_0 = 0$ at $t = t_0 = 0$, means that the constant of integration is

$$C \quad = \quad 0 \tag{B.19}$$

and the explicit form for s is

$$s \quad = \quad -\ 25\ v_{P\text{-}P} \sqrt{5}\ t^3\ (t\ -\ \tau)^3\ /\ 6\tau^5 \tag{B.20}$$

The stationary points for s are given by

$$t \quad = \quad 0 \quad \text{(twice)} \qquad \text{for a local minimum} \tag{B.21a}$$

$$t \quad = \quad \tau/2 \qquad \text{for a local maximum} \tag{B.21b}$$

$$t \quad = \quad \tau \quad \text{(twice)} \qquad \text{for a local minimum} \tag{B.21c}$$

from which the corresponding values are

$$s_{MAX} \quad = \quad 25\ v_{P\text{-}P}\ \tau \sqrt{5}\ /\ 384 \tag{B.22}$$

and $$s_{MIN} \quad = \quad 0 \tag{B.23}$$

The range of s is simply

$$s_{P\text{-}P} \quad = \quad s_{MAX}\ -\ s_{MIN}$$

$$= \quad 25\ v_{P\text{-}P}\ \tau \sqrt{5}\ /\ 384 \tag{B.24}$$

Reasonable, and slightly exaggerated, estimates for the peak-to-peak velocity in the side impact of interest to this study are

$$v_{P\text{-}P} = 8 \;\&\; 13 \text{ kph} \quad [= 5 \;\&\; 8 \text{ mph}] \qquad \text{(B.25)}$$

to the nearest whole number. Typical values for the duration τ of such a low severity side impact are of the order of

$$\tau = 200 \text{ msec} \quad \text{(say)} \qquad \text{(B.26)}$$

which is selected for both values of $v_{P\text{-}P}$ in equation (B.25).

The consequences of equations (B.25) and (B.26) are illustrated in Figure B.1 for the smaller value of $v_{P\text{-}P}$ and in Figure B.2 for the larger value of $v_{P\text{-}P}$. The values of $a_{P\text{-}P}$ in Figures B.1(a) and B.2(a) are

$$a_{P\text{-}P} = 7.2 \;\&\; 11.5 \text{ g} \qquad \text{(B.27)}$$

which coincides with calculations of equation (B.17). The appropriate level of accuracy for these calculated values is one decimal place. The form of a in these figures has

$$t[a_{MAX}] = 23 \;\&\; 177 \text{ msec}; \quad t[a_{MIN}] = 100 \text{ msec} \qquad \text{(B.28)}$$

for both $v_{P\text{-}P}$, thus matching the times derived from equation (B.14). The times for the extrema in v in Figures B.1(b) and B.2(b) are

$$t[v_{MAX}] = 55 \text{ msec}; \quad t[v_{MIN}] = 145 \text{ msec} \qquad \text{(B.29)}$$

in agreement with equation (B.06).

Similarly, the values of $s_{P\text{-}P}$ in Figures B.1(c) and B.2(c) coincide with calculations of equation (B.24), namely

$$s_{P\text{-}P} = 6.5 \;\&\; 10.4 \text{ cm} \quad [= 2.6 \;\&\; 4.1 \text{ in}] \qquad \text{(B.30)}$$

corresponding to $v_{P\text{-}P}$ = 8.0 & 16.0 kph, respectively. Again, values are quoted to one decimal place as an appropriate level of accuracy.

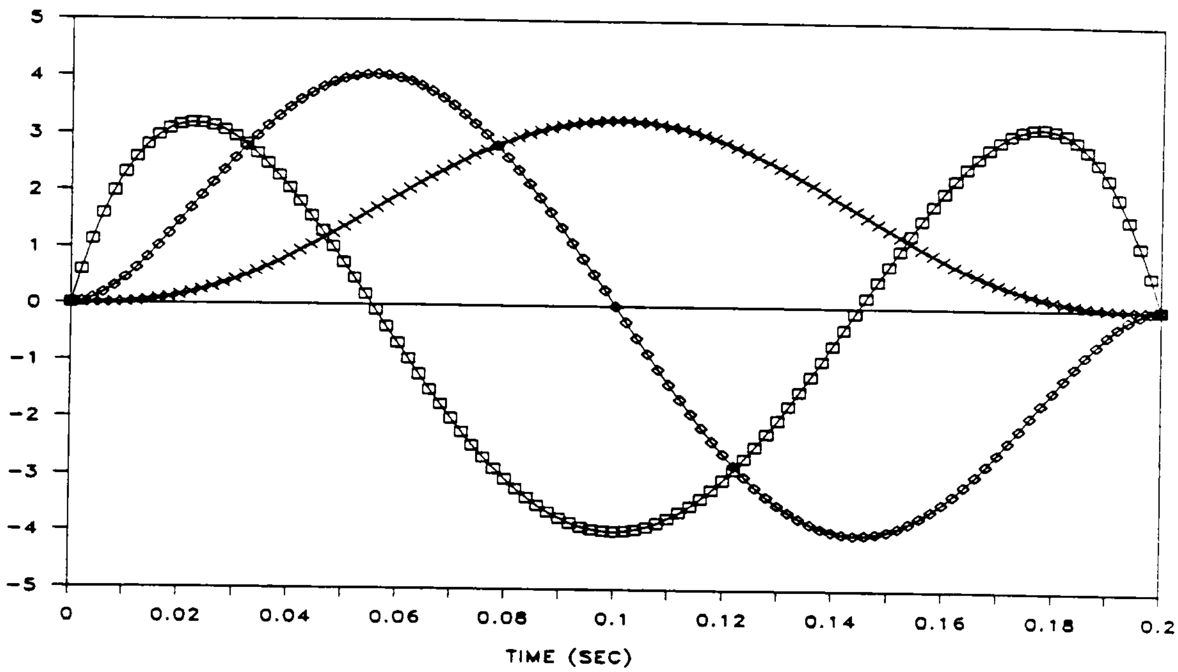

Figure B.1 *Time history for side impact with v_{P-P} = 8 kph [5 mph]: (a) acceleration □, g; (b) velocity ◇, kph; and, (c) displacement ×, cm/2*

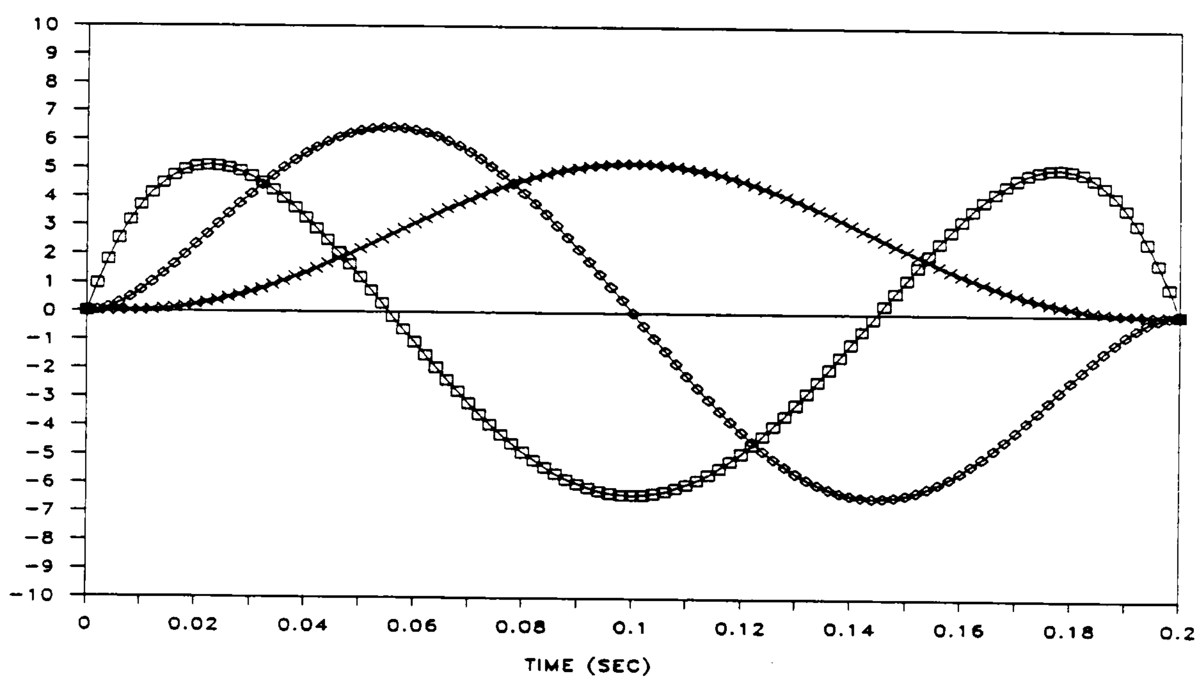

Figure B.2 *Time history for side impact with v_{P-P} = 13 kph [8 mph]: (a) acceleration □, g; (b) velocity ◇, kph; and, (c) displacement ×, cm/2*

Footnote

It should be noted that functional forms other than the polynomials discussed in Appendices A and B can be fitted to the boundary conditions in Tables A.1 and B.1. However, the results calculated in these appendices are so straightforward that it is difficult to see how the reasonable values can be improved upon. This is reinforced by the appearance of the figures in both appendices, none of which contains any irregularities or discontinuities.

An example of the alternative methods employed for the sake of completeness is the consideration of various sinusoidal functions for the apparently periodic nature of v in Tables A.1 and B.1. These functions are not as easy to manipulate as those used above and they are not explored further because they offer no obvious benefit over the above.

Acknowledgments

It is a pleasure for the author to record his appreciation and gratitude to Ed Mulligan of Edge Associates, Silver Spring, Maryland, for his support and encouragement of this research.

"Because the foolishness of God is wiser than men; and the weakness of God is stronger than men."[46]

References

1. Shaibani, S.J., "The SJSATBPC package: mainframe-quality results with the Crash Victim Simulation in the microcomputer environment." Seventeenth International Workshop on Human Subjects for Biomechanical Research, Washington, DC, October 4, 1989, U.S. Department of Transportation, Washington, DC.

2. Shaibani, S.J., "The development of the SJSATBPC microcomputer package to obtain mainframe-accuracy with the Crash Victim Simulation analysis of occupant kinematics." Paper presented at 42nd Annual Meeting of American Academy of Forensic Sciences, Cincinnati, OH, February 19-24, 1990.

3. McHenry, R.R., and Naab, K.N., "Computer simulation of the automobile crash victim - A validation study." Report YB-2126-V-1R, Calspan Corporation, Buffalo, NY, July 1966.

4. Segal, D.J., and McHenry, R.R., "Computer simulation of the automobile crash victim - Revision No. 1." Report VJ-2492-V-1, Calspan Corporation, Buffalo, NY, March 1968.

5. Kidd, E.A., "Development of physical and analytical simulating of the automobile crash victim." Report VJ-2554-V-1, Calspan Corporation, Buffalo, NY, December 1970.

6. Bartz, J.A., "A three dimensional computer simulation of a motor vehicle crash victim." Report VJ-2978-V-1, Calspan Corporation, Buffalo, NY, July 1971.

7. Fleck, J.T., Butler, F.E., and Vogel, S.L., "An improved three-dimensional computer simulation of motor vehicle crash victims." Report ZQ-5180-L-1, Calspan Corporation, Buffalo, NY, 1974.

8. Fleck, J.T., Butler, F.E., and Vogel, S.L., "An improved three-dimensional computer simulation of crash victims - Volume 1: Engineering manual." Publication DOT HS 801 507, U.S. Department of Transportation, Washington, DC, April 1975. (Available through NTIS, Springfield, VA 22161, via Accession No. PB-241 692.)

9. Fleck, J.T., Butler, F.E., and Vogel, S.L., "An improved three-dimensional computer simulation of crash victims - Volume 2: Model validation." Publication DOT HS 801 508, U.S. Department of Transportation, Washington, DC, April 1975. (Available through NTIS, Springfield, VA 22161, via Accession No. PB-241 693.)

10. Fleck, J.T., Butler, F.E., and Vogel, S.L., "An improved three-dimensional computer simulation of crash victims - Volume 3: User's manual." Publication DOT HS 801 509, U.S.

Department of Transportation, Washington, DC, April 1975. (Available through NTIS, Springfield, VA 22161, via Accession No. PB-241 694.)

11. Fleck, J.T., Butler, F.E., and Vogel, S.L., "An improved three-dimensional computer simulation of crash victims - Volume 4: Programmer's manual." Publication DOT HS 801 510, U.S. Department of Transportation, Washington, DC, April 1975. (Available through NTIS, Springfield, VA 22161, via Accession No. PB-241 695.)

12. Fleck, J.T., and Butler, F.E., "Development of an improved computer model of the human body and extremity dynamics." Report AFAMRL-TR-75-11, Armstrong Medical Research Laboratory, Wright Patterson Air Force Base, Dayton, OH, July 1975.

13. Shaibani, S.J., "A uniform input data convention for the Cal 3-D Crash Victim Simulation." Report 1419/82, Oxford University Engineering Laboratory, England, July 1982.

14. Shaibani, S.J., "Application of the Cal 3-D CVS program to evaluate the equilibrium position of an Euler-jointed Alderson Part572." Report 1426/82, Oxford University Engineering Laboratory, England, August 1982.

15. Shaibani, S.J., "Review of CVS work conducted at Oxford University between June 1982 and September 1982." Report 1427/82, Oxford University Engineering Laboratory, England, September 1982.

16. Shaibani, S.J., "The modelling of occupant response in collisions of $\Delta v = 30$ mph with different principal directions of force from 0° to 30°." Report 1456/83, Oxford University Engineering Laboratory, England, February 1983.

17. Shaibani, S.J., and Digges, K.H., "Analytical reconstructions of front seat passenger response in a road accident." Report 1457/83, Oxford University Engineering Laboratory, England, March 1983.

18. Digges, K.H., and Shaibani, S.J., "Analytical reconstructions of driver response in a road accident." Report 1458/83, Oxford University Engineering Laboratory, England, April 1983.

19. Shaibani, S.J., "The reconstruction of vehicle occupant response in road traffic accidents." Film made at Computing Teaching Centre, University of Oxford, England, 1983. [Presented at Seventeenth International Workshop on Human Subjects for Biomechanical Research, Washington, DC, October 4, 1989.]

20. American Association for Automotive Medicine (AAAM), "The Abbreviated Injury Scale, 1980 Revision." AAAM, Morton

Grove, IL, 1980.

21. American Association for Automotive Medicine (AAAM), "The Abbreviated Injury Scale, 1985 Revision." AAAM, Morton Grove, IL, 1985.

22. Shaibani, S.J., "Energy management in the distribution of injuries incurred by automotive occupants under different types of restraint condition." Paper presented at 42nd Annual Meeting of American Academy of Forensic Sciences, Cincinnati, OH, February 19-24, 1990.

23. Shaibani, S.J., "Distribution of injuries received with different types of seat-belt use." Film made in Arlington, VA, 1989. [Presented at 42nd Annual Meeting of American Academy of Forensic Sciences, Cincinnati, OH, February 19-24, 1990.]

24. Federal Register, 31, 15212, Washington, DC, December 3, 1966.

25. Federal Register, 32, 2408, Washington, DC, February 3, 1967.

26. Federal Register, 35, 16927, Washington, DC, November 3, 1970.

27. Federal Register, 36, 4600, Washington, DC, March 10, 1971.

28. Federal Register, 37, 12393, Washington, DC, June 23, 1972.

29. Federal Register, 37, 22871, Washington, DC, October 26, 1972.

30. Federal Register, 42, 34299, Washington, DC, July 5, 1977.

31. Collins, J.C., "Accident Reconstruction." Charles C. Thomas, Springfield, IL, 1979.

32. Rivers, R.W., "Traffic Investigators' Handbook." Charles C. Thomas, Springfield, IL, 1980.

33. Rivers, R.W., "On-Scene Traffic Accident Investigators' Manual." Charles C. Thomas, Springfield, IL, 1981.

34. Rivers, R.W., "Traffic Accident Investigators' Book of Formulae and Tables." Charles C. Thomas, Springfield, IL, 1981.

35. Grime, G., "Handbook of Road Safety Research." Butterworths, London, England, 1987.

36. Society of Automotive Engineers (SAE), "Accident Reconstruction: State-of-the-Art." Publication SP-733, SAE, Warrendale, PA, 1988.

37. Adapted from Sieg, K.W., Scott, A.D., and Adams, S.P., "Illustrated Essentials of Musculoskeletal Anatomy." Center for Allied Health Instructional Personnel, University of Florida, Gainesville, FL, 1977.

38. Leetch, B.D., and Bowman, W.L., "Articulated total body (ATB) VIEW package software report - Volume 1." Armstrong Medical Research Laboratory Report AFARML-TR-81-111, Wright Patterson Air Force Base, Dayton, OH, October 1981.

39. Leetch, B.D., and Bowman, W.L., "Articulated total body (ATB) VIEW package software report - Volume 2." Armstrong Medical Research Laboratory Report AFARML-TR-81-111, Wright Patterson Air Force Base, Dayton, OH, October 1981.

40. Shaibani, S.J., "Variations in neck injuries produced by similar loading conditions." Film made at Department of Mathematics, Liberty University, Lynchburg, VA, 1991. [Presented at Nineteenth International Workshop on Human Subjects for Biomechanical Research, San Diego, CA, November 17, 1991.]

41. McElhaney, J.H., Roberts, V.L., and Hilyard, J.F., "Handbook of Human Tolerance." Japan Automobile Research Institute, Ibaraki, Japan, 1976.

42. Society of Automotive Engineers (SAE), "Human Tolerance to Impact Conditions as Related to Motor Vehicle Design -- SAE J885 APR 80." SAE, Warrendale, PA, April 1980.

43. Mertz, H.J., and Patrick, L.M., "Investigation of the kinematics and kinetics of whiplash." Paper 670919 in Proceeding [*sic*] of Eleventh Stapp Car Crash Conference, Anaheim, CA, October 10-11, 1967, pp. 267-317, Society of Automotive Engineers, New York, NY.

44. Mertz, H.J., and Patrick, L.M., "Strength and response of the human neck." Paper 710855 in Proceedings of Fifteenth Stapp Car Crash Conference, Coronado, CA, November 17-19, 1971, pp. 207-255, Society of Automotive Engineers, New York, NY.

45. Patrick, L.M., and Chou, C.C., "Response of the human neck in flexion, extension and lateral flexion." Report No. VRI7.3, Society of Automotive Engineers (SAE) Vehicle Research Institute, SAE, Warrendale, PA, April 16, 1976.

46. The Holy Bible, The First Epistle of Paul the Apostle to the Corinthians, Chapter 1, verse 25, The King James Version, 1611.

DISCUSSION

PAPER: **Disparate Cervical Trauma in Low Severity Insults**

SPEAKER: Saami Shaibani, Liberty University

QUESTION: Carly Ward, Biodynamics Engineering

Well Saami, I hate to discourage you but, based on your data, I wouldn't be here today. My company is running 5mph, 10mph, 15mph impacts on fully human, fully-instrumented human volunteers with 9 accelerometers on their heads, accelerometers on their spines at T-1 and L-5. We're doing these impacts because we're interested in the same phenomenon you were looking at here; Are people being injured? And, I hate to tell you this, but we didn't even get an ache or a pain. The response you're predicting does look like part 572, unfortunately, that isn't the human response. And then the hybrid 3 response is a little better but it too lacks the bio-fidelity at these speeds. So I wouldn't take these numbers too seriously because I 've ridden this ride at least 3 times and didn't even get a headache, so I think you should rethink the idea that people are getting injured at these low speeds.

A: I'm not saying they're injured, Carly, that's not what I've said. I' m saying if we use this measure of 200, which is the threshold of discomfort, a threshold of pain.

Q: I didn't have any pain; I wasn't in any pain and we were at much higher speeds.

A: I accept that, but this is for a particular vehicle geometry for a particular occupant. We've seen 5 times out of 6 that the values are very low and then we have this discrepancy, that doesn't mean that the person was injured, what it does suggest, on a comparative basis, is that that 6th case is more likely to produce an injury than those other 5. I'm not saying that that number 6 produces an injury and I said at the beginning that I recognize the severe limitations of part 572; I recognize the severe limitations of hybrid 3; what I'm saying is, if we use those as some kind of benchmark...

Q: But what I'm saying is this isn't real, this is not anywhere near real, so if you're making a calculation on something that's a computer simulation that bears no semblance to reality, you can't expect to get a number that's even close to real. I'm telling you that I've had 7 people ride these runs fully MRI'ed before the run, fully MRI'ed after the run; there is nothing happening to these people and we're in light cars. We're producing a lot of damage on these cars, not the damage you're talking about, minuscule damage, this is real damage and I hate to see you saying this because it's misleading the people here. People are not getting injured at these speeds.

A: I'm not saying they are, Carly.

Q: That was my interpretation of what you were saying, that you were getting minute injuries and that we should be concerned about this. And what I'm saying is you're not getting an injury.

A: I think we're saying the same thing. If you use CVS, with its limitations; if you use whatever ATD that you do with its limitations, you can set up some kind of comparative study, not an accident study; you will need field data like that which you are generating as some kind of real world bench mark. But within those assumptions, comparatively, those first five (runs) there's absolutely no probability of injury unless there are some very, very unusual circumstances like a frail old lady for example. If we can eliminate those first 5, then that 6th one stands out. Does that mean that there's an injury? No it doesn't-what it does suggest is that the mythical value of 200lbs may not be a good descriptor.

Q: You are missing my point. What I'm saying is you have an idealization here that doesn't represent the real world, doesn't represent an individual, barely represents an out-of-date dummy, and you're trying to take a number from that and make it meaningful. And it doesn't work that way; if you've got a gross difference in response, you've got a gross difference in numbers and you just can't make those correlations.

A: Were you seeing those kind of excursions in the upper parts of the body?

Q: You can see that on the part 572 because it has a very stiff neck and in the hybrid-3 you get a little more neck motion, but on a real person you have them folding over the belt and a lot of stretch forward which is entirely different and you're getting about 10g's on the human and we're not getting that g on the dummy because the dummy is just riding it different and you're not getting the head motion that you're getting in a real person. If I tried to make a calculation from a dummy it wouldn't be anywhere near what the human is at these speeds. The dummy is designed for higher impact.

A: The work that you've done can be used as a kind of mechanism to calibrate these kinds of numbers and it's going to be easier to do these rounds on the computer whichever device you happen to use to get a handle on it, not an exact final answer but to have a step in the right direction, possibly.

Q: Priya Prasad, Transportation Research Center

How did you calculate the delta-v or the vehicle velocities from the real world accidents which you were investigating?

A: That was separately calculated by other people. I just took their result and plugged that in.

Q: I could hazard a guess; one of the ways to calculate that would be to use the CRASH3 computer program which is not known to be very accurate for really low severity accidents, so that your delta-v's which you used may not be very accurate in representing the real world accident.

A: I recognize that there is going to be a lot of discrepancy at low speed with any type of calculation of delta-v.

Q: Guy Nusholtz, Chrysler

I have two questions: How did you calculate or approximate the seat deformation that occurs in the rear impacts?

A: The first one uses well-defined off-the-shelf mechanical descriptors for seats, forced deflection functions, and so on that have been measured historically.

Q: Did you have them for the individual seats that you were simulating?

A: No, but for similar types of seats for similar types of vehicles. Not exactly that seat; not exactly that vehicle.

Q: To follow-up Carly's statement: as I interpret what you're saying is, if you're able to get a response parameter to use in the model in the CVS model, then you might be able to get some useful information out of it. Is that correct?

A: You put it much better than I did, yes sir.

Q: So, in fact, this is just sort of an exercise to show what might be done and the results don't really have any significance. They just give you a clue as to how we might address it using a CVS model.

A: That is absolutely correct and I'm going to ask you to present my next paper.